

Mathematical Morphology in Polar-Logarithmic Coordinates. Application to Erythrocyte Shape Analysis

Miguel A. Luengo-Oroz¹, Jesús Angulo¹,
Georges Flandrin², and Jacques Klossa³

¹ Centre de Morphologie Mathématique, Ecole des Mines de Paris,
35 rue Saint-Honoré, 77305 Fontainebleau, France

² Unité de Télémedecine, Hôpital Universitaire Necker, 149 rue de Sèvres, 75743 Paris

³ TRIBVN Company, Paris, France
{luengo,angulo}@cmm.ensmp.fr, Francegflandrin@wanadoo.fr,
jklossa@tribvn.com

Abstract. We present in this paper the application of mathematical morphology operators through a transformation of the Cartesian image into another geometric space, i.e. pol-log image. The conversion into polar-logarithmic coordinates as well as the derived cyclic morphology provides satisfying results in image analysis applied to round objects or spheroid-shaped 3D-object models. As an example of application, an algorithm for the shape analysis of the shape of red blood cells is given.

1 Introduction

A fundamental advantage of mathematical morphology [9] applied to image processing is that it is intuitive since it works directly on the spatial domain: the structuring elements considered as the “basic bricks” play the same role as frequencies do in the analysis of the sound. However, by using the discrete metrics and grids, which are more or less close to the Euclidian ones, we can not achieve the desired results when working on round objects.

It has been frequently suggested that the image should be transformed to other domains which would be adapted to the nature of the object or to the analysis that must be carried out (i.e. Fourier descriptors). This paper (extracted from [7]) proposes to use mathematical morphology operators through a transformation of the image into another geometric space that would present an intuitive nature. Therefore, we try to find a representation system which would present more advantages than the traditional Cartesian representation when processing and analyzing images which contain some kind of radial symmetry, or in general, which have “a center”. The selected transformation is the polar-logarithmic representation (or log-pol coordinates [12]). This mapping has already been used to map the visual cortex of primates [10] (the photoreceptors of the retina are placed according to the same organization). Thus, this model of “log-pol fovea” is applied mainly to the artificial vision systems of robots [3], for which the need

for real time processing of the visual information gives rise to the same problem regarding resource-optimization that the human visual system encounters. In addition, due to its scientific utility in describing fundamental aspects of human vision, the artificial “fovea” has been applied in order to assess the optical flow, to encode narrowband video, or else to recognize and track objects [2].

2 Log-Pol Coordinates

2.1 Definition

The polar-logarithmic transformation converts the original image (x, y) into another (ρ, ω) in which the angular coordinates are placed on the vertical axis and the logarithm of the radius coordinates are placed on the horizontal one (furthermore a normalization has to be carried out in order to implement the transformation), see Fig. 1(a). More precisely, with respect to a central point (x_c, y_c) : $\rho = \log(\sqrt{(x - x_c)^2 + (y - y_c)^2})$, $0 \leq \rho \leq \rho_{max}$; $\omega = \arctan(\frac{y - y_c}{x - x_c})$, $0 \leq \omega < 2\pi$.

pseudocode direct transformation $(x, y) \implies (\rho, \omega)$

for $\rho = 1 : R$ {; for $\omega = 1 : W$ {;
 $x = \frac{\Delta X_{max}}{R} R^{\frac{\rho}{R}} \cos(\frac{2\pi\omega}{W}) + X_{central}$; $y = \frac{\Delta Y_{max}}{R} R^{\frac{\rho}{R}} \sin(\frac{2\pi\omega}{W}) + Y_{central}$
ImageValue $(\rho, \omega) = \text{ImageValue}(f(x, y))$ } }

2.2 Properties

Rotation. Because of the periodic nature of the angular component, rotations in the original Cartesian image become vertical cyclic shifts in the transformed log-pol image.

Scaling. The changes of size in the original image become horizontal shifts in the transformed image, according to the autosimilarity property of the exponential function, i.e. λ is the scale factor, $r' = \lambda r \implies \rho' = \log \lambda r = \log \lambda + \log r = cte + \rho$.

Choice of a Center. Due to the definition of the pol-log image, the choice of the center (x_c, y_c) is crucial. In fact, all the algorithms are sensitive to variations of the center, since the existence of a center is the principal prerequisite for all further developments. If the center point is not previously defined by the nature of the object, the choice of the center of gravity as central point is deemed adequate for most of cases.

If the goal is to analyze extrusions, the maximum of the distance function from the binary mask (the ultimate eroded set) can be considered as a satisfactory choice. This center maximizes the inscribed circumference within the object, however the main drawback is that this maximum can be multiple (set of regional maxima). In general, a better choice would correspond to the geodesic center defined as the minimum of the propagation function (if the set has no hole the propagation function reaches its minimum value at a unique point) [6].

3 Cyclic Morphology

3.1 Definition

Let $f(x, y)$ be an image defined on the discrete space $E \subset Z^2$, $(x, y) \in (Z \times Z)$, with values of the complete lattice \mathcal{T} (for simplicity the complete lattice is considered to be $\mathcal{T} = Z$ or a subset from Z corresponding to the grey levels $\mathcal{T} = \{0, 1, \dots, 255\}$). The extension of the operators from classical mathematical morphology to the log-pol representation is achieved by changing the support of the image in order to introduce the principle of periodicity. The log-pol transformation of the function $f(x, y)$ generates a new function image $\hat{f}(\rho, \omega) : E_{\rho, \omega} \rightarrow \mathcal{T}$, where the support of the image is the space $E_{\rho, \omega}$, $(\rho, \omega) \in (Z \times Z_p)$ and where the angular variable $\omega \in Z_p$ is periodic with period p equivalent to 2π . A new relation of neighborhood is established where the points at the top of the image ($\omega = 0$) are neighbors to the ones at the bottom of the image ($\omega = p - 1$), therefore the edge connection should only take into account in the radial direction. The image can be seen as a strip where the superior and the inferior borders are joined, see Fig. 1(b).



Fig. 1. (a) Example of conversion $(x, y) \rightarrow (\rho, \omega)$ ((x_c, y_c) corresponds to the body center of the crab). (b) Dilatation of one point by a square in log-pol coordinates.

The aim of this change is to preserve the invariance with respect to rotations in the Cartesian space, when morphological operations are done in the log-pol space, see an example in Fig. 2.

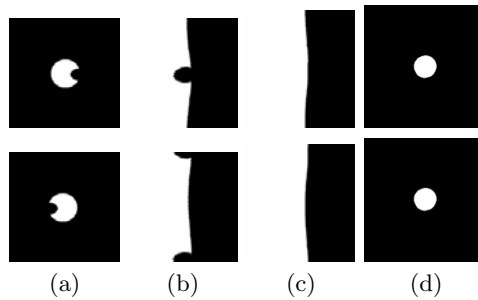


Fig. 2. (a) Original and 180° rotation, (b) Direct transformation: pol-log, (c) Closing using as SE a centered square, (d) Invert transformation: Cartesian.

3.2 Implementation

In order to implement the new neighborhood relation and to be able to use morphological operators, two possibilities are considered:

- Modify the neighborhood relation and the basics operators code (erosion, dilation, etc.) by adding the operator “module of the size of the image in the direction of the cyclic coordinate”. So if (ρ, ω) corresponds to the (x, y) axes, “ y ” should be substituted by “ $y \bmod(y_{max})$ ” for the whole code.
- Extend the image along its angular direction by adding the top part of the image onto the bottom and the bottom part onto the top. The size of the vertical component from each part should be bigger than the size of the vertical component of the structuring element in order to avoid a possible edge effect. After having “cycled the image”, morphological operators should be applied as usual and only the image corresponding to the initial mask should be kept. In Fig. 3 an illustrative example is shown. With this system all the existing code is recyclable.

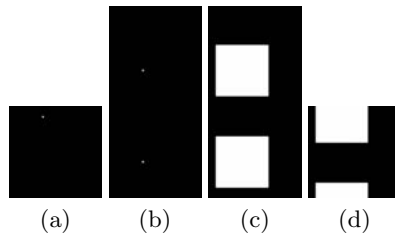


Fig. 3. Example of 2D Cyclic dilation: (a) Original , (b) “Cycled image”, (c) Dilation by a square, (d) Original image mask: cyclic dilation.

3.3 Meaning of the Structuring Elements

The use of classic structuring elements (SE) in the log-pol image is equivalent to the use of “radial - angular” structuring elements in the original image. A vertical structuring element corresponds to an arc in the original image and a square corresponds to a circular sector (see fig. 4). For all the examples here presented, the center of the SE corresponds to the central point.

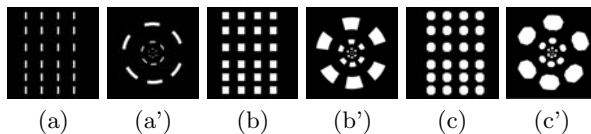


Fig. 4. Pol-log structuring elements (a,b,c) and their equivalence in the Cartesian space(a',b',c'). For all these exemples (x_c, y_c) is the central point of the image.

It is worth noting the fact that horizontal and vertical neighborhoods respectively acquire radial and angular sense in the original image; for instance, the transformation from a circumference is a vertical straight line.

4 Tools

Once cyclic morphology is defined, all the classic operators from mathematical morphology can be applied, giving at first view very interesting results for a certain kind of images. Some examples are given below.

4.1 Circular Filtering

One of the immediate applications is a method for extracting inclusions or extrusions from the contour of a relatively rounded shape with simple openings or closings [9]. The proportion of the vertical size of the structuring element with respect to the whole vertical size represents the angle affected in the original Cartesian image. With respect to a classical extraction in Cartesian coordinates, the choice of size is not as critical, making this a very advantageous point. It is due to the large zone plate in the openings/closings spectrum that is always found after a determined value (until the complete elimination of the object).

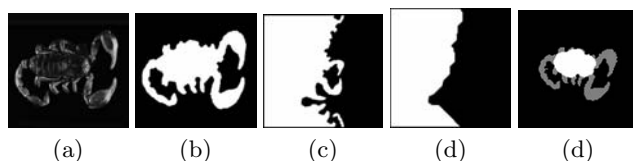


Fig. 5. Extremities segmentation from “Leiurius quinquestriatus”: (a) Original, (b) Binary mask, (c) Log-pol transformation ((x_c, y_c) corresponds to the body center), (d) Opening with a vertical structuring element sized 20% of the whole image (i.e. 72°), (e) Invert transformation.

4.2 Radial Skeleton

Let g be an image with only a connected component object. Let \hat{g} be the log-pol transformation of g . If the chosen center to transformation $g \rightarrow \hat{g}$ is inside the object, the frontier of the object in \hat{g} goes from the top of the image ($\omega = 0^\circ$) to the bottom ($\omega = 360^\circ$), and the connected component region resulting from the transformation of the object remains on the left of the edge ($\rho < \rho_{edge}$). If we apply an homotopic thinning [8] to \hat{g} (according to the cyclic neighborhood); a skeleton is obtained mainly in the horizontal direction. This construction, when coming back to the Cartesian space, makes the skeleton to acquire a radial sense.

Therefore, we define a *radial inner skeleton* as the skeleton obtained by an homotopic thinning from the log-pol transformation of an objet. The invert transformation to Cartesian coordinates from the branches of the radial inner skeleton has radial sense and tends to converge on the center ($\rho = 0$). We also define the *radial outer skeleton* as the skeleton obtained by an homotopic thinning from the inverted image of the log-pol transformation of an object. The invert transformation to Cartesian coordinates from the branches of the radial outer skeleton has radial sense and this time, they tend to diverge to an hypothetical circumference in the infinity ($\rho \rightarrow \infty$), see examples given in Fig. 6 and 8.

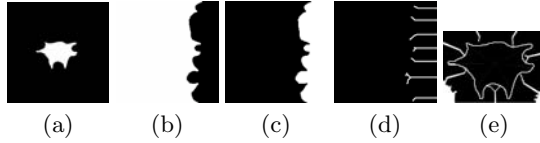


Fig. 6. Radial outer Skeleton: (a) Original , (b) Log-pol transformation (c) Inverted image , (d) Thinning, (e)Results in cartesian space.

5 Erythrocyte Shape Analysis: Inclusions and Extrusions Extraction Algorithm

In hematology, the visual analysis of the morphology of erythrocytes (size, shape, color, center,...) is of vital importance as it is well known that anomalies and variations from the typical red blood cell are associated with anemia or other illnesses [4]. In Fig. 7 a selection of abnormal erythrocytes is shown. We present hereafter one of the algorithms dedicated to the shape analysis developed in the MATCHCELL2 project [7], [1]. The aim of this algorithm is to extract the inclusions or extrusions from the erythrocyte shape, which is ideally round.

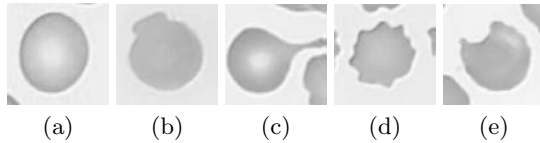


Fig. 7. (a) Normal erythrocyte, (b) “Mushroom” erythrocyte, (c) “Spicule” erythrocyte , (d) “Echinocyte” erythrocyte, (e) “Bitten” erythrocyte.

5.1 Algorithm

An algorithm for the extraction of extrusions and the identification of “mushroom” class is presented. It starts with the binary mask of the segmented erythrocyte, image (A), and the results correspond to image (G), see Fig. 8). If $(G) \neq \emptyset$ and the verifications are confirmed, it is classified as “mushroom” erythrocyte (we have considered the gravity center as the center of the log-pol transformation).

1° / Log-pol transformation from (A) \Rightarrow (B). 2° / Radial inner skeleton from (B) \Rightarrow (C). 3° / Circular filtering: Residue from a vertical opening of 120° (maximal admissible angle for the extrusion) from (B) \Rightarrow (D)=extrusion candidates. 4° / Geodesic reconstruction from (D) using as markers $(D) \cap (C) \Rightarrow$ (E). 5° / Biggest connected set from (E) \Rightarrow (F). We verify that $[Surface(F) > \mu_1 Surface(E)]$. 6° / We verify that two branches of (D) reconstruct (F). 7° / We verify that $[Surface(F)/sizeimage > \mu_2]$. 8° /Invert transformation from (F) to Cartesian coordinates \Rightarrow (G)¹.

¹ μ_1 and μ_2 are fixed experimentally to 0.75 and 0.005.

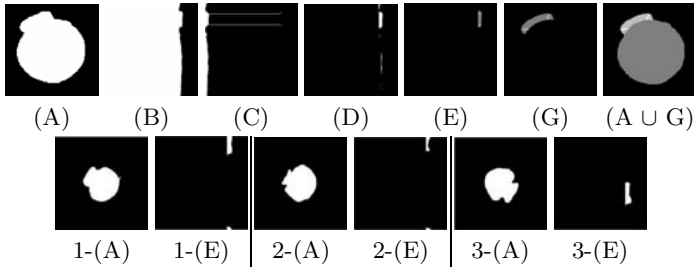


Fig. 8. Upper row, extrusion extraction algorithm for “mushroom” erythrocytes. Lower row, other examples of “mushroom” extraction (1,2,3).

Moreover, an analogous algorithm in order to extract the inclusions has been developed by applying the *radial outer skeleton* (step 2), and a closing instead of an opening (step 3).

5.2 Validation of the Approach

The algorithm has an efficient and robust performance in the extraction of inclusions and extrusions. The use of the skeleton in order to sieve the candidates gives much greater robustness than would a mere opening or closing. This procedure refines small connected components preselected as deformations. Furthermore, the examples corresponding to “bitten”, “spicules” and “mushroom” have been correctly classified (see more examples and details in [7]).

6 Conclusions and Perspectives

The fundamental idea here presented is that the conversion of the image into another intuitive geometric representation can provide advantages over the traditional Cartesian representation. Regarding mathematical morphology, the key issue is to obtain structuring elements that are adapted to the nature of the objects to be analyzed, not by deforming them, but by transforming the image itself. The conversion into polar-logarithmic coordinates as well as the derived cyclic morphology appears to be a field that may provide satisfying results in image analysis applied to round objects or spheroid-shaped 3D-object models [7]. Basically, we have presented binary image processing and some of its basic tools, however the study of more complex morphological operators still remains, as well as a deeper developing of image processing for grey-scale or color.

Acknowledgements

We gratefully thank the “Groupe Français d’Hématologie Cellulaire” for supporting this study.

References

1. Angulo, J. (2003) *Morphologie mathématique et indexation d'images couleur. Application à la microscopie en biomédecine*. Ph.D. Thesis, Ecole des Mines de Paris.
2. Bernardino, A. and Santos-Victor, J. and Sandini, G.(2002) *Model Based Attention Fixation Using Log-Polar Images*, "Visual Attention Mechanisms", Plenum Press
3. Bolduc, M. and Levine, M. (1998) *A review of biologically motivated space-variant data reduction models for robotic vision*, CVIU, 69(2): 170–184.
4. Bronkorsta, P. and Reinders, M. (2000) *On-line detection of red blood cell shape using deformable templates*, Pattern Recognition Letters 21,413-424
5. Klossa J., G. Flandrin et J. Hemet. (2002) *Teleslide: better slide representativeness for digital diagnostic microscopy applications*.
6. Lantuejoul, C. et Maisonneuve, F. *Geodesic methods in quantitative image analysis*. Pattern Recognition, 17(2) : 177–187, 1984.
7. Luengo Oroz, M.A. (2004) *Morphologie mathématique en coordonnées logarithmique-polaires et méthodes géométriques de classification. Application à l'étude des érythrocytes*. Master Thesis. Ecole des Mines de Paris.
8. Meyer, F.(1989) Skeletons and perceptual graphs. *Signal Processing*, 16 : 335–363.
9. Serra, J. (1982, 1988) *Image Analysis and Mathematical Morphology. Vol I & II*, Academic Press, London.
10. Schwartz, E. (1977) *Spatial mapping in the primate sensory projection : Analytic structure and relevance to perception*, Biological Cybernetics, 25:181–194.
11. Vincent, L.(1992) *Morphological area openings and closings for grayscale images*. In Proc. NATO Shape in Picture Workshop, Driebergen, Springer-Verlag.
12. Weiman, C. and Chaikin, G. (1979) *Logarithmic spiral grids for image processing and display*. Comp Graphics and Image Proc, 11:197–226.